Yao *et al. Animal Diseases* (2024) 4:20
https://doi.org/10.1186/s44149-024-00125-y

Animal Diseases

ORIGINAL ARTICLE

Open Access

Lactobacillus alleviates intestinal epithelial barrier function through GPR43-mediated M2 macrophage polarization

Yong Yao[1], Yuhan Zhang[1], Mengzhen Song[1], Jinping Fan[1], Shengkai Feng[1], Jingjing Li[1], Zhifeng Wu[1], Bo Zuo[1], Shiyu Tao[1] and Xiangdong Liu[1*]

Abstract

Lactobacillus species have excellent abilities to reduce intestinal inflammation and enhance gut barrier function. This study elucidated the potential mechanisms through which *Lactobacillus* mitigates lipopolysaccharide (LPS)-induced intestinal injury from the perspective of macrophage–intestinal epithelial cell interactions. *Lactobacillus* intervention improved the histopathological score; elevated ZO-1 and Occludin protein production; reduced $CD16^+$ cell numbers; diminished IL-1β, IL-6, and TNF-α levels; decreased inducible nitric oxide synthase (iNOS) expression; increased $CD163^+$ cell numbers; elevated IL-10 concentration; and increased arginase-1 (Arg1) expression in LPS-challenged piglets. *Lactobacillus* pretreatment also altered the colonic microbiota, thereby increasing the butyric acid concentration and GPR43 expression in the LPS-challenged piglets. Compared with those in the LPS group, sodium butyrate (SB) pretreatment decreased IL-1β, IL-6 and TNF-α secretion and iNOS expression but increased IL-10 secretion and Arg1 expression in macrophages. The SB-pretreated macrophages reduced the protein expression of TLR4, MyD88, and phosphorylated NF-κB p65 but increased the protein expression of ZO-1 and Occludin in intestinal epithelial cells. Moreover, GLPG0974 blocked the beneficial effects of SB on macrophages and intestinal epithelial cells. This study demonstrated that *Lactobacillus* improves intestinal barrier function by regulating the macrophage phenotype through the control of butyric acid and GPR43 levels to further control inflammation.

Keywords *Lactobacillus*, Butyric acid, GPR43, Macrophage, Gut barrier

Introduction

Early life is a critical period for intestinal development when the intestinal mucosal immune system and intestinal epithelial barrier function gradually develop. Poorly developed immune function of the intestinal mucosa can directly lead to defects in intestinal development (Gensollen et al. 2016; Xia et al. 2022). The intestinal inflammatory response is a major factor in impairing intestinal epithelial barrier function, and proinflammatory cytokine overproduction disrupts the expression of tight junction proteins, thereby impairing intestinal epithelial barrier function (Chen et al. 2021). Macrophages contribute to intestinal barrier integrity or the maintenance of intestinal homeostasis by secreting various pro- or anti-inflammatory cytokines to regulate the inflammatory response (Na et al. 2019; Viola and Boeckxstaens 2021). The local microenvironment in vivo induces macrophages to activate and differentiate into M1 macrophages, the inflammatory phenotype, and M2 macrophages, the anti-inflammatory phenotype (Quail et al. 2016). Macrophages of different phenotypes have distinct

Handling editor: Shuai Wang.

*Correspondence:
Xiangdong Liu
liuxiangdong@mail.hzau.edu.cn
[1] College of Animal Sciences and Technology, Huazhong Agricultural University, Wuhan 430070, China

functions; therefore, altering the macrophage phenotype and thus regulating their biological functions is crucial for reducing the occurrence of intestinal inflammation (Sica et al. 2015).

G protein-coupled receptor 43 (GPR43), which is expressed on M2 macrophages but not on M1 macrophages, is activated by short-chain fatty acids (SCFAs), a vital metabolite produced by the intestinal microbiota. GPR43 is involved in inflammatory response regulation (Macia et al. 2015; Vieira et al. 2015; Kimura et al. 2020). The plant extract alleviated intestinal inflammation by inhibiting M1 macrophage polarization while enhancing M2 macrophage polarization in mice. This was accompanied by an increase in SCFA-producing bacteria, a substantial upregulation of intestinal mucosal GPR43, and the expression of tight junction proteins in mice (Xia et al. 2020). In mice, lithium carbonate protects against ulcerative colitis by upregulating SCFA-producing bacteria and altering the SCFA profile, but its protective effect against colitis was lost in GPR43 knockout mice (Huang et al. 2022). Thus, GPR43 is an intermediate mediator of the phenotypic transformation of macrophages, and SCFA-stimulated GPR43 promotes macrophage differentiation toward the M2 anti-inflammatory phenotype, regulates the development of intestinal inflammation, and thus improves intestinal epithelial barrier function.

Probiotics can improve the intestinal microbiota structure, regulate intestinal mucosal immunity, and maintain intestinal epithelial barrier function (Chen et al. 2017a; Rodriguez-Sorrento et al. 2021). The SCFA–GPR43 axis is crucial for protecting the intestinal barrier after probiotic intake (Xie et al. 2022). Our recent study reported that *Lactobacillus* is the dominant genus with the highest relative abundance in the piglet intestine and that *Lactobacillus* deficiency may contribute to diarrheal disease development in piglets (Li et al. 2023b). *Limosilactobacillus johnsoni (L. j)* and *Limosilactobacillus mucosae (L. m)* exert beneficial effects on the development and maturation of the host immune system (Ayyanna et al. 2018; Yang et al. 2020). In another recent study, *L. j* and *L. m* modified macrophage polarization by secreting extracellular vesicles to mitigate intestinal inflammatory injury (Li et al. 2023a). However, whether *L. j* and *L. m* protect host intestinal health by modulating the SCFA-GPR43-M2 macrophage–gut barrier axis remains unclear.

Pigs are similar to humans in terms of anatomy, genetics, and physiology. They are therefore often used as translational models for studying gastrointestinal inflammatory diseases (Meurens et al. 2012; Wang et al. 2021). Lipopolysaccharide (LPS)-induced inflammation models are commonly used for the immunological characterization of pigs (Wyns et al. 2015; Liu et al. 2021). Therefore, we first used an LPS-challenged piglet model to determine the effects of *L. j* and *L. m* on the intestinal microbiota, SCFA production, GPR43 expression, macrophage phenotype, and intestinal barrier function. Furthermore, the potential mechanisms through which *L. j* and *L. m* exert anti-inflammatory effects and augment intestinal barrier function were further analyzed in terms of SCFA–macrophage–intestinal epithelial cell interactions.

Results

Lactobacillus enhances colonic barrier function in LPS-challenged piglets

To explore the protective effect of *Lactobacillus* on colonic barrier function in LPS-challenged piglets, piglets were gavaged with *Lactobacillus* for 14 d and then treated with LPS for 4 h (Fig. 1A). We first observed the morphological structure of the colon in the four piglet groups. H&E staining revealed a disruption cellular damage, and glandular separation in the colonic epithelium of the LPS-challenged piglets but not in piglets of the CON, LPS + *L. j*, or LPS + *L. m* group piglets (Fig. 2A). According to the histopathological examination, the LPS-challenged piglets had a greater pathological score in the colonic epithelium than did the CON group piglets, whereas the LPS + *L. j* and LPS + *L. m* groups had significantly lower pathological scores than the LPS group ($P < 0.05$; Fig. 2B). Moreover, ZO-1 and Occludin protein expression was significantly lower in the colon in the LPS group than in the CON group, whereas ZO-1 and Occludin protein levels were effectively restored in the LPS + *L. j* and LPS + *L. m* groups ($P < 0.05$; Fig. 2C–E).

Lactobacillus regulates colonic macrophage polarization in LPS-challenged piglets

To reveal the role of *Lactobacillus* in modulating the colonic macrophage phenotype in LPS-challenged piglets, we examined macrophage polarization status using a variety of methods. Immunohistochemical staining was performed to observe macrophage polarization markers in the colon of the four piglet groups. The proportions of $CD16^+$ cells (a M1 macrophage marker) was higher and $CD163^+$ cells (a M2 macrophage marker) was lower in the LPS group than in the CON group (Fig. 3A). In contrast, the levels of these markers in the LPS + *L. j* and LPS + *L. m* groups were restored close to those in the CON group ($P < 0.05$). The LPS-challenged piglets had significantly higher levels of IL-1β, IL-6, and TNF-α in the colon than did the CON piglets, whereas the IL-10 levels were lower ($P < 0.05$) (Fig. 3B–E). IL-6 level was significantly lower, while IL-10 was higher in the LPS + *L.j* group than in the LPS group ($P < 0.05$). The IL-1β, IL-6, and TNF-α levels were markedly lower in the LPS + *L.m* group than in the LPS group, whereas the IL-10 levels

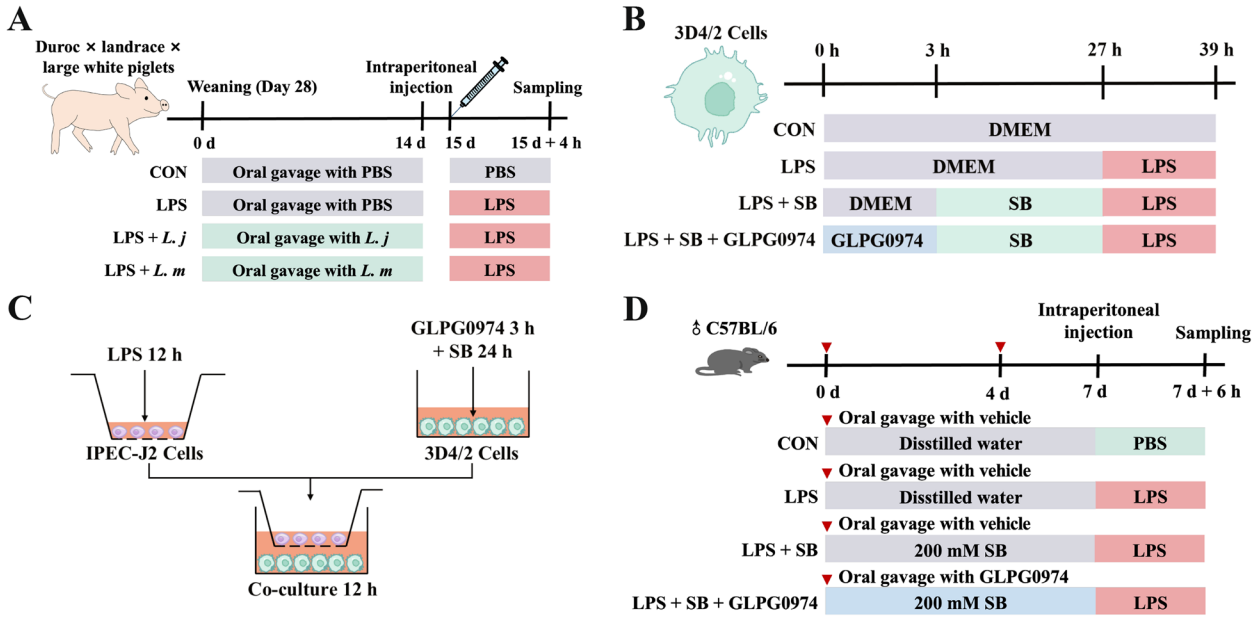

Fig. 1 The experimental design of this study. **A** in vivo *piglet experiments*. **B** in vitro *macrophage experiment*. **C** Coculture experiment of macrophages and intestinal epithelial cells in vitro. **D** in vivo mouse experiments. CON, control; DMEM, Dulbecco's modified Eagle's medium; *L. j*, *Limosilactobacillus johnsoni*; *L. m*, *Limosilactobacillus mucosae*; LPS, lipopolysaccharide; PBS, phosphate buffer saline; SB, sodium butyrate

were higher ($P<0.05$). Compared with the CON group, the LPS group had significantly more protein expression of inducible nitric oxide synthase (iNOS) but dramatically lower protein expression of arginase-1 (Arg1) and GPR43. In contrast, the *L.j* or *L.m* interventions restored these indicators to normal levels ($P<0.05$; Fig. 3F–I).

Lactobacillus shifts the colonic digesta microbiota in LPS-challenged piglets

To observe the effects of *Lactobacillus* on the intestinal microbiota of LPS-challenged piglets, we performed 16S rRNA sequencing and bioinformatics analysis of the colonic digesta. Supplemental Fig. 1A–C presents the microbial α diversity of the colonic digesta samples from the four piglet groups. The observed ACE and Shannon indices of the colonic digesta microbiota in the four groups were similar ($P>0.05$). Principal coordinate analysis (PCoA) based on Bray–Curtis distances revealed that the microbial community structure of the colonic digesta in the four groups was somewhat different ($P=0.053$; Supplemental Fig. 1D). Firmicutes, Bacteroidota, and Actinobacteriota were the most dominant phyla in the colonic digesta (Supplemental Fig. 1E). *Blautia*, *Subdoligranulum* and *Clostridium_sensu_stricto_1* were the most dominant genera in the CON piglets (Supplemental Fig. 1F). *Clostridium_sensu_stricto_1*, *Terrisporobacter*, and *Prevotella* were the most dominant genera in the LPS-treated piglets (Supplemental Fig. 1F). *Terrisporobacter*, *Clostridium_sensu_stricto_1* and *Blautia* were the most dominant genera in the LPS+*L. j* piglets (Supplemental Fig. 1F). *Blautia*, *Clostridium_sensu_stricto_1* and *Catenibacterium* were the most predominant genera in the LPS+*L. m* piglets (Supplemental Fig. 1F). Seven differential bacteria were identified between the CON and LPS groups (Supplemental Fig. 2A). Compared with the CON group, the LPS group had seven enriched bacteria (*Intestinibacter_spp*, *Senegalimassilia_spp*, *Prevotellaceae_UCG-003_spp* and 4 *Prevotella_spp*). Six differential bacteria were also identified between the LPS and LPS+*L.j* groups (Supplemental Fig. 2B). The LPS+*L. j* group had 1 enriched bacterium (*Clostridia_UCG-014_spp*) and five depleted bacteria (*[Ruminococcus]_torques_group_spp*, *Olsenella_spp*, *Senegalimassilia_spp*, *Prevotella_spp* and *UCG-005_spp*). Seventeen differential bacteria were identified between the LPS and LPS+*L.m* groups (Supplemental Fig. 2C). The LPS+*L.m* group had nine enriched bacteria (two *Catenibacterium_spp*, *Olsenella_spp*, *Bifidobacterium_spp*, *Blautia_spp*, *Rikenellaceae_RC9_gut_group_spp*, and three *Mitsuokella_spp*) and eight depleted bacteria (three *Terrisporobacter_spp*, *_Romboutsia_spp*, *Senegalimassilia_spp*, *Prevotella_spp*, *Prevotellaceae_NK3B31_group_spp* and *UCG-005_spp*).

Lactobacillus alters the colonic SCFA profile in LPS-challenged piglets

To observe the effect of Lactobacillus on the production of intestinal microbial metabolites in LPS-challenged

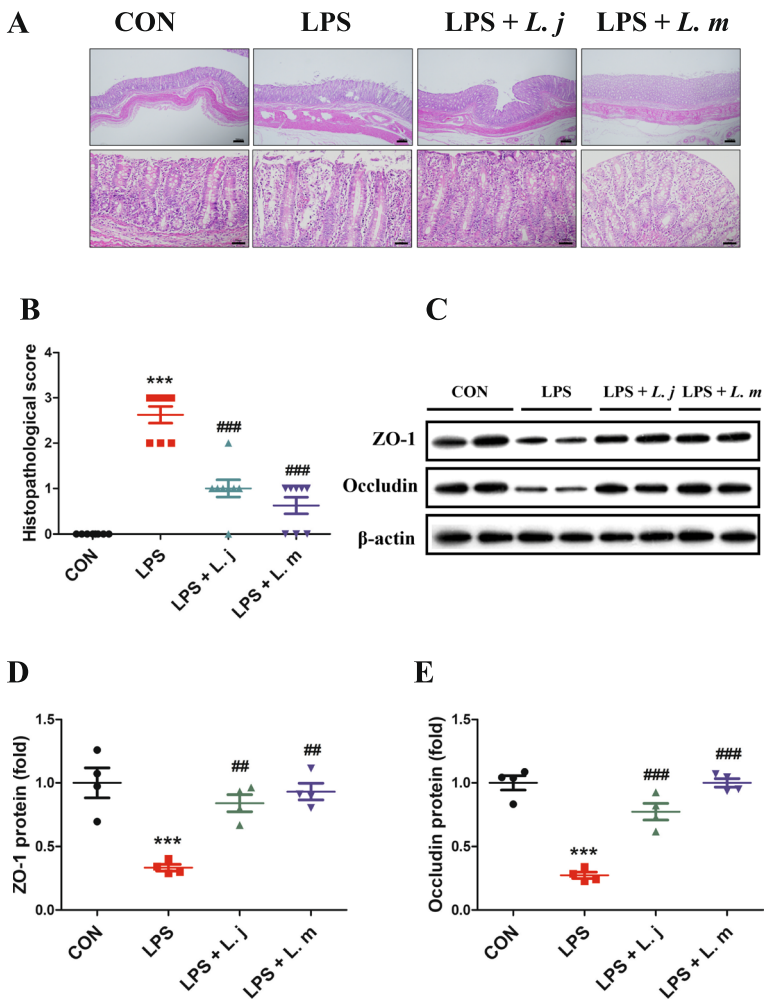

Fig. 2 Effect of *L.j* or *L.m* on colonic barrier function in LPS-challenged piglets. **A** Colonic morphological structure after H&E staining. Images of colonic morphology (scale bar = 200 or 50 μm). **B** Colonic histopathological score. **C** Colonic ZO-1 and Occludin protein expression. Colonic ZO-1 (**D**) and Occludin (**E**) protein expression analysis. The data are presented as the means ± SEMs ($n = 8$ for **A** and **B**; $n = 4$ for **C**–**E**). Differences between the LPS and CON groups, ***$P < 0.001$. Differences between the LPS + *L. j* or LPS + *L. m* group and the LPS group, ##$P < 0.01$; ##$P < 0.001$. CON, control; H&E, hematoxylin and eosin; *L. j*, *Limosilactobacillus johnsoni*; *L. m*, *Limosilactobacillus mucosae*; LPS, lipopolysaccharide

piglets, we examined the SCFA content in the colonic digesta. The lactic acid, acetic acid, and propionic acid concentrations in the four piglet groups were similar ($P > 0.05$; Fig. 4A–C). The butyric acid level was significantly lower in the LPS-challenged piglets than in the control piglets, whereas it was obviously greater in the LPS + *L. j* or LPS + *L. m* group than in the LPS group ($P < 0.05$; Fig. 4D). A correlation analysis was performed between the butyric acid content and the relative abundance of differentially abundant bacteria. The butyric acid content was positively correlated with one and negatively correlated five differential bacteria in the LPS and LPS + *L. j* groups (Fig. 4E), positively correlated with nine and negatively correlated with eight differential bacteria in the LPS and *L.m* groups (Fig. 4F).

SB regulates macrophage polarization and tight junction protein expression in intestinal epithelial cells through GPR43 activation

To determine the role of the predominant butyric acid in piglet colonic digesta in the regulation of macrophage polarization and its underlying mechanisms, we used SB and GLPG0974 (a specific inhibitor of GPR43) to treat macrophages in vitro (Fig. 1B). The IL-1β, IL-6 and TNF-α levels in the 3D4/2 cell supernatant were obviously higher and IL-10 level was lower in the LPS group *vs* CON group, whereas they showed the exact opposite trend in LPS + SB group *vs* LPS group ($P < 0.05$; Fig. 5A–D). IL-1β, IL-6 and TNF-α levels were significantly higher in the LPS + SB + GLPG0974 group *vs* LPS + SB group, whereas the IL-10 level was lower ($P < 0.05$;

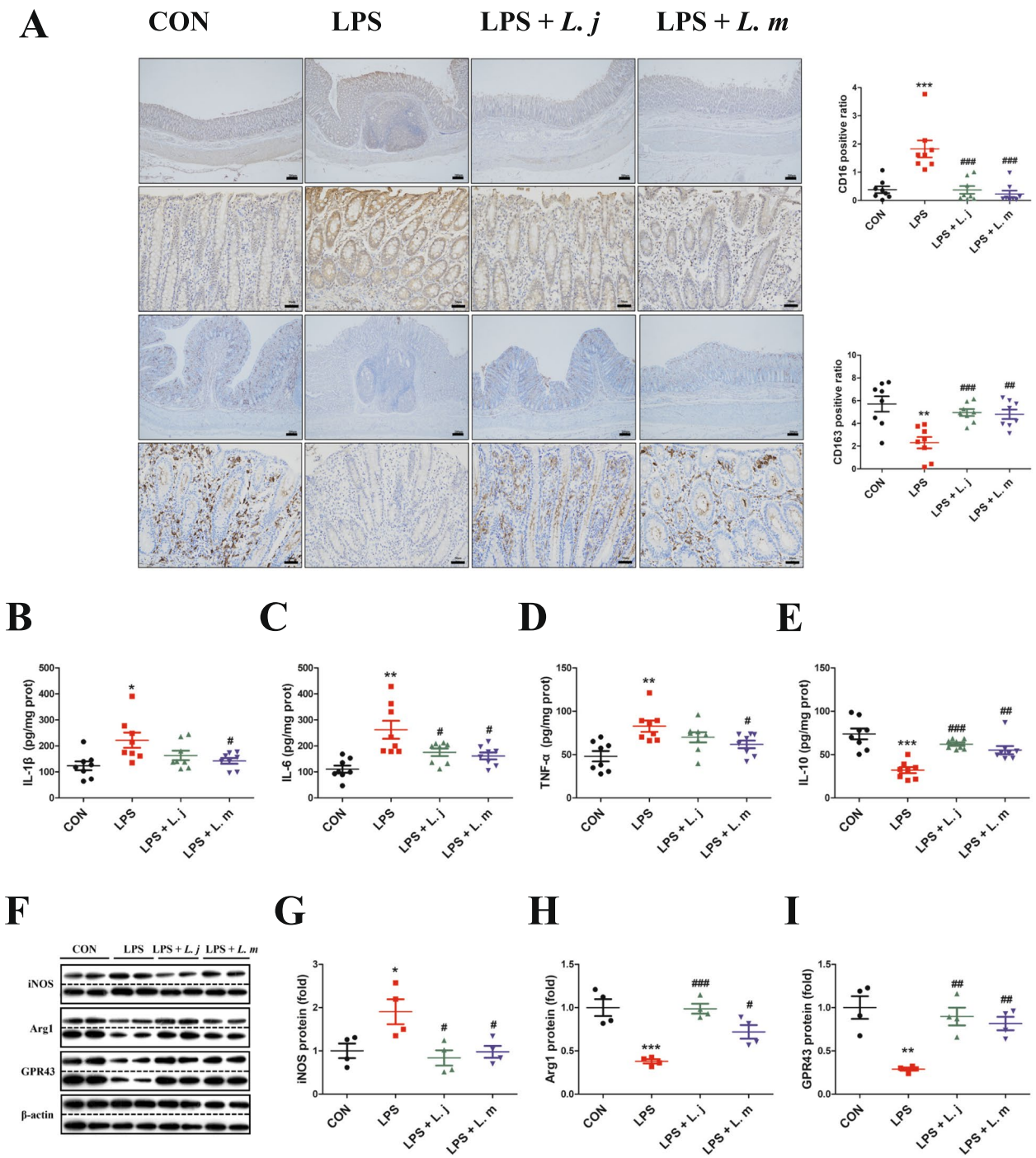

Fig. 3 Effect of *L.j* or *L.m* on colonic macrophage polarization in LPS-challenged piglets. **A** Colonic CD16 and CD163 expression after IHC staining. Images of colonic CD16 and CD163 expression (scale bar = 200 or 50 μm). CD16- and CD163-positive ratio analysis. Colonic levels of IL-1β (**B**), IL-6 (**C**), TNF-α (**D**), and IL-10 (**E**). (**F**) Images showing colonic iNOS, Arg1, and GPR43 protein expression. Colonic iNOS (**G**), Arg1 (**H**), and GPR43 (**I**) protein expression quantification. The data are presented as the means ± SEMs ($n = 8$ for **A**–**E**; $n = 4$ for **F**–**I**). Differences between the LPS and CON groups, $^{*}P < 0.05$; $^{**}P < 0.01$; $^{***}P < 0.001$. Differences between the LPS + *L.j* or LPS + *L.m* group and the LPS group, $\#P < 0.05$; $\#\#P < 0.01$; $\#\#\#P < 0.001$. Arg1, arginase-1; CON, control; GPR, G protein-coupled receptor; IHC, immunohistochemistry; IL, Interleukin; *L. j*, *Limosilactobacillus johnsoni*; *L. m*, *Limosilactobacillus mucosae*; iNOS, inducible nitric oxide synthase; LPS, lipopolysaccharide; TNF, tumor necrosis factor

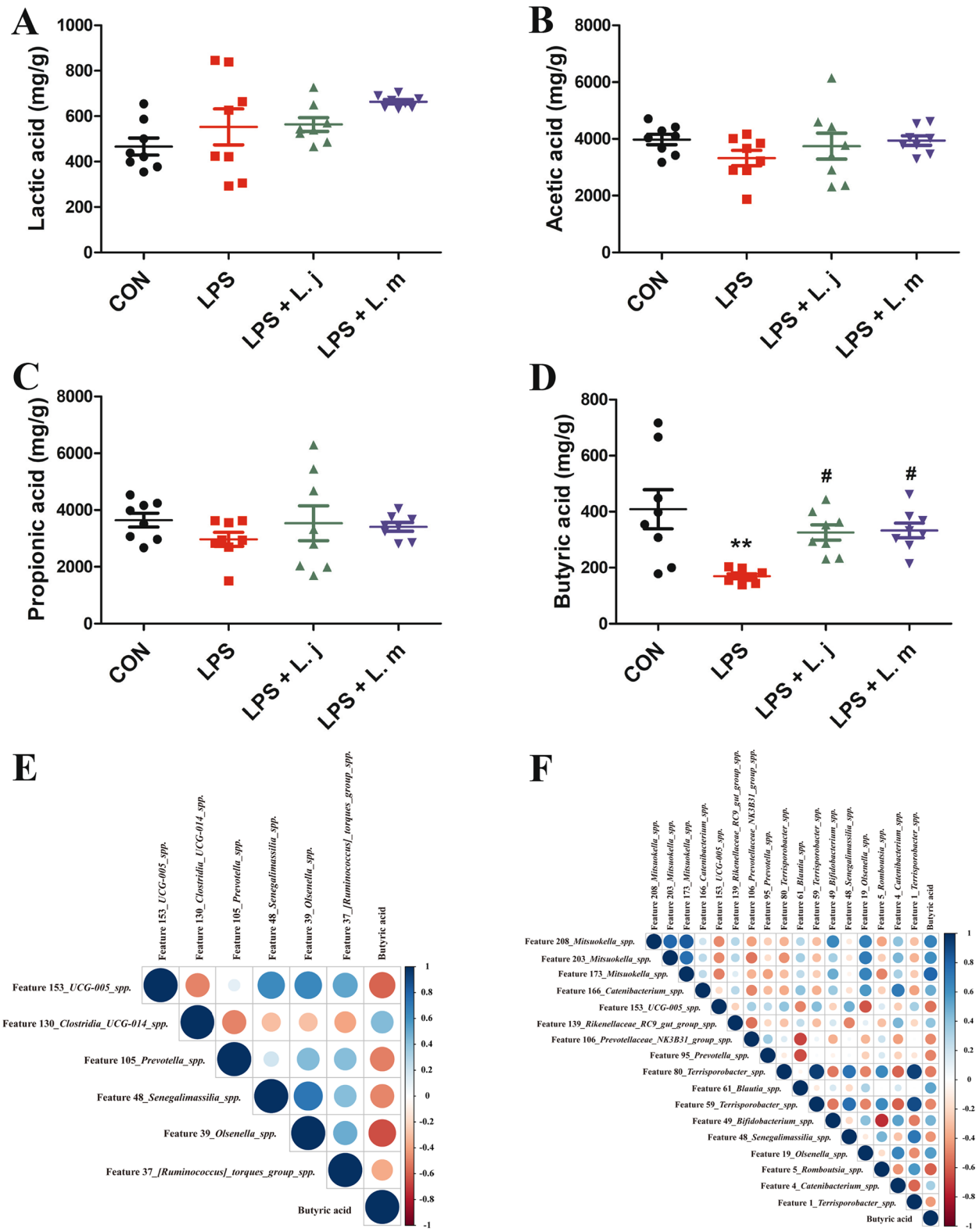

Fig. 4 Effect of *L.j* or *L.m* on the colonic SCFA profile in LPS-challenged piglets. Colonic lactic acid (**A**), acetic acid (**B**), propionic acid (**C**), and butyric acid (**D**) concentrations. Correlation analysis of differential bacteria in the colonic digesta with butyric acid concentration in the *L. j* (**E**) and *L. m* (**F**) intervention groups. The data are presented as the means ± SEMs ($n = 8$). Differences between the LPS and CON groups, $^{**}P < 0.01$. Differences between the LPS + *L. j* or LPS + *L. m* group and the LPS group, $\#P < 0.05$. CON, control; *L. j*, *Limosilactobacillus johnsoni*; *L. m*, *Limosilactobacillus mucosae*; LPS, lipopolysaccharide

Fig. 5A–D). The *iNOS* and *Arg1* expression levels were greater and lower, respectively, in the LPS group *vs* CON group and LPS + SB + GLPG0974 group *vs LPS + SB group* ($P < 0.05$) (Fig. 5E and F). The iNOS and Arg1 gene expression levels were lower and greater, respectively, in the LPS + SB group than in the LPS group ($P < 0.05$). *ZO-1* and *Occludin* expression was lower in the LPS group *vs* CON group and in the LPS + SB + GLPG0974 group *vs* LPS + SB group whereas they were higher ($P < 0.05$; Fig. 5G and H).

In intestinal epithelial cells, SB-treated macrophages enhance tight junction protein expression by inhibiting the TLR4 signaling pathway

To elucidate the role of SB-pretreated macrophages in regulating the intestinal epithelial cell barrier, we constructed a coculture system of SB-pretreated macrophages and LPS-pretreated intestinal epithelial cells in vitro (Fig. 1C). The expression of GRP43 and Arg1 was detected in 3D4/2 cells from coculture systems which showed a significant upregulation ($P < 0.05$) in the SB-pretreated 3D4/2 cells compared with that in the CON group (Fig. 6B and C). The expression of GPR43 and Arg1 protein decreased in 3D4/2 cells with the combination pretreatment of GLPG0974 and SB compared with that in the SB pretreatment ($P < 0.05$) (Fig. 6B and C). The TLR4 signaling pathway and tight junction protein expression were examined in IPEC-J2 cells which cocultured with 3D4/2 cell (Fig. 6D). As shown in Fig. 6E–I, TLR4, MyD88, and p-NF-κB p65 decreased ($P < 0.05$), whereas ZO-1 and Occludin increased in the SB-pretreated IPEC-J2 cells compared with the CON group. Compared with the SB pretreatment group, the GLPG0974 and SB combinaton groups exhibited increased TLR4, MyD88, and p-NF-κB p65 protein expression but decreased ($P < 0.05$) ZO-1 and Occludin protein abundance in IPEC-J2 cells.

SB enhances colonic barrier function in LPS-challenged mice

To further validate the effect of SB on intestinal barrier function in LPS-challenged mammals, we used mice as a model and injected LPS after pretreatment with SB or GLPG0974 (Fig. 1D). The body weight change was significantly lower in the LPS group than that in the CON group, which was reversed by the SB intervention (Fig. 7A). Treatment with a GPR43 inhibitor reversed the mitigating effect of SB. No significant difference ($P > 0.05$) in colon length was noted among the CON, LPS, and LPS + SB groups. In contrast, the colon length of the LPS + SB + GLPG0974 group mice was significantly shorter ($P < 0.05$) than that of the LPS + SB group mice (Fig. 7B and C). SB treatment diminished the disruption of the colonic morphological structure in LPS-challenged mice, whereas GLPG0974 attenuated the effect of SB (Fig. 7D). *ZO-1* and *Occludin* expression was significantly higher ($P < 0.05$) in the LPS + SB group than in the LPS group, whereas it was significantly lower ($P < 0.05$) in the LPS + SB + GLPG0974 group than in the LPS + SB group (Fig. 7E and F).

SB regulates colonic macrophage polarization and the TLR4 signaling pathway in LPS-challenged mice

To verify the mechanism by which SB regulates macrophage polarization and intestinal epithelial barrier function, we detected the expression of macrophage markers and the colonic TLR4 signaling pathway in mice. The LPS + SB group had significantly lower IL-1β, IL-6, and TNF-α levels in the colon than that in the LPS group, whereas the IL-10 level was higher ($P < 0.05$). The IL-1β, IL-6, and TNF-α concentrations were markedly higher in the LPS + SB + GLPG0974 group than that in the LPS + SB group, whereas the IL-10 level was lower ($P < 0.05$; Fig. 8E–J). Moreover, the LPS + SB group had significantly lower *iNOS*, *TLR4*, *MyD88* and *NF-κB* mRNA expression in the colon than the LPS group, whereas the expression of *Arg1* and *GPR43* were greater ($P < 0.05$). The *iNOS*, *TLR4*, *MyD88*, and *NF-κB* expression levels were markedly higher in the LPS + SB + GLPG0974 group than in the LPS + SB group, whereas the *Arg1* and *GPR43* expression levels were lower ($P < 0.05$; Fig. 8E–J).

Discussion

Impairment of intestinal epithelial barrier function caused by the intestinal inflammatory response severely affects the physical and mental health of patients and the sustainable development of the livestock industry (Di Tommaso et al. 2021; Tang et al. 2022). The mechanism of intestinal epithelial barrier damage must be elucidated from the perspective of regulating the intestinal inflammatory response. The nutritional intervention program should be optimized to improve intestinal epithelial

(See figure on next page.)

Fig. 5 Effect of SB or GLPG0974 coincubation on macrophage polarization in 3D4/2 cells. The concentrations of IL-1β (**A**), IL-6 (**B**), TNF-α (**C**), and IL-10 (**D**) in the 3D4/2 cell supernatant. The mRNA expression of *iNOS* (**E**) and *Arg1* (**F**) in 3D4/2 cells. The mRNA expression of *ZO-1* (**G**) and *Occludin* (**H**) in IPEC-J2 cells. The data are presented as the means ± SEMs ($n = 6$). Differences between the LPS and CON groups, ***$P < 0.001$. Differences between the LPS + SB group and the LPS group, ###$P < 0.001$. Differences between the LPS + SB + GLPG0974 group and the LPS + SB group, &&&$P < 0.001$. Arg1, arginase-1; CON, control; IL, interleukin; iNOS, inducible nitric oxide synthase; LPS, lipopolysaccharide; SB, sodium butyrate; TNF, tumor necrosis factor

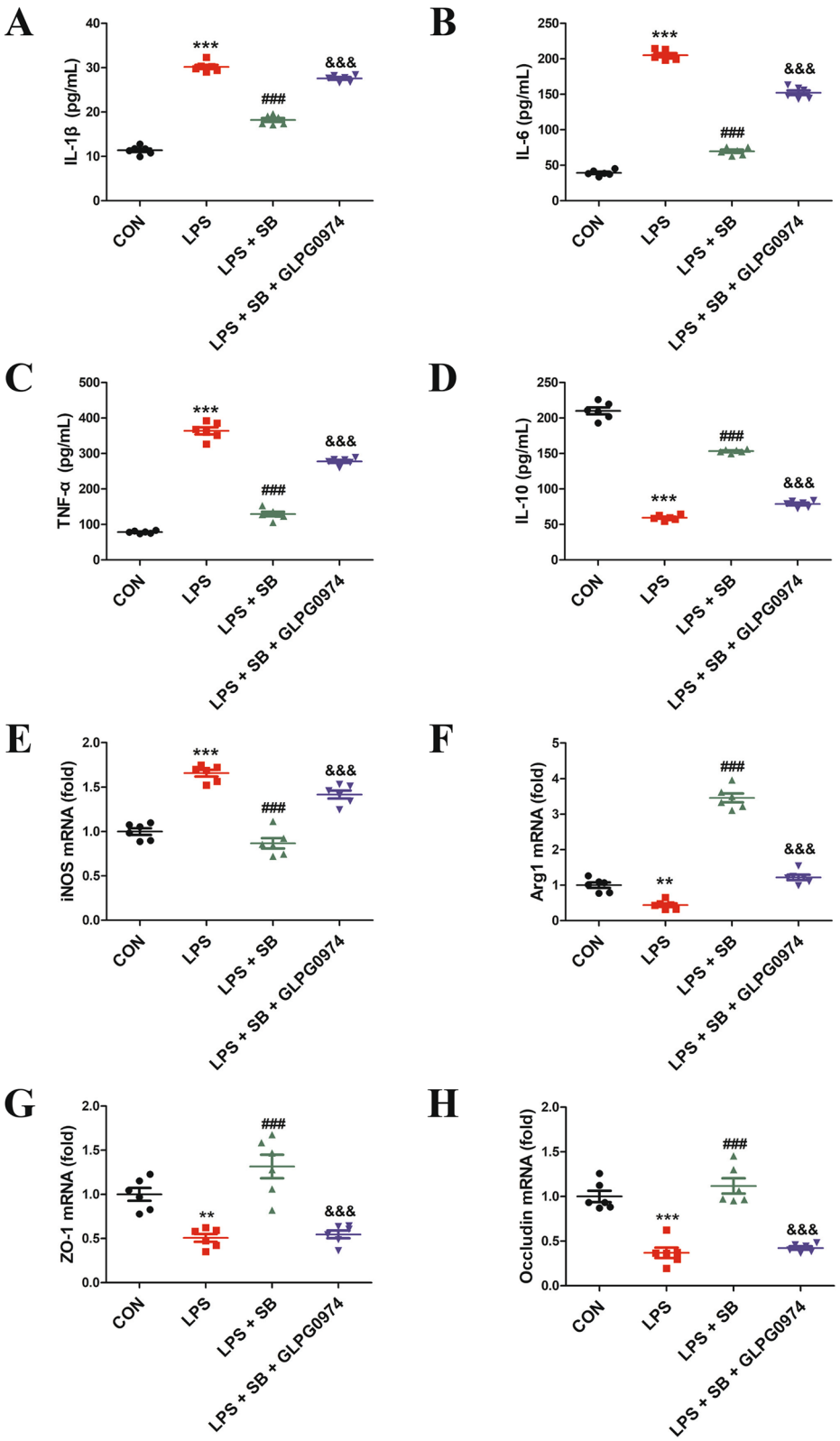

Fig. 5 (See legend on previous page.)

barrier function. Because of its excellent anti-inflammatory properties, *Lactobacillus* has been extensively used in clinical therapeutic and animal husbandry (Ayyanna et al. 2018; Li et al. 2019; Hu et al. 2021). In the present study, *Lactobacillus* (*L. j* and *L. m*) reshaped the intestinal microbiota, augmented butyric acid production and GPR43 expression, regulated the macrophage phenotype and increased intestinal tight junction protein expression. In vitro experiments revealed the ability of SB to modulate macrophage polarization. Furthermore, SB-pretreated macrophages inhibited the expression of the TLR4 signaling pathway and elevated tight junction protein expression in intestinal epithelial cells. Notably, the GPR43 inhibitor blocked these beneficial effects of SB. Mouse experiments verified the protective effect exerted by the SB–GPR43–M2 macrophage axis on the intestinal barrier.

The LPS-induced inflammatory response in the gut is good for studying immunomodulation (Cui et al. 2019; Mao et al. 2020). In this study, LPS-challenged piglets had impaired colonic morphology, increased pathological scores, elevated proinflammatory macrophage proportions, decreased anti-inflammatory macrophage proportions, and reduced tight junction protein expression. Changes in these biological indicators were consistent with those of a previous study (Wang et al. 2022) and suggested that we successfully established an experimental intestinal inflammation model in piglets. Intestinal macrophages, located in the mucosal lamina propria beneath the intestinal epithelium, can identify various signals in the intestinal environment, thereby modifying their phenotype and performing the corresponding immune functions (Bain and Mowat 2014; Isidro and Appleyard 2016). M1 macrophage activation can increase LPS-induced intestinal epithelial cell death and inflammatory cytokine secretion, augment intestinal mucosal permeability, and decrease the transmembrane resistance of intestinal epithelial cells. M2 macrophage activation effectively inhibits IL-1β, IL-6, and TNF-α release from intestinal epithelial cells, increases the transmembrane resistance of these cells, and promotes epithelial cell repair (Han et al. 2022). In mice, *Lactobacillus* alleviates colitis by activating anti-inflammatory macrophage polarization (Jia et al. 2022; Fu and Wu 2023). Our data revealed that the *L. j* and *L. m* interventions resulted in macrophage differentiation from the M1 proinflammatory phenotype to the M2 anti-inflammatory phenotype, thus inhibiting the secretion of proinflammatory cytokines and increasing the secretion of anti-inflammatory cytokines.

A stable intestinal microbiota is a crucial player in the clearance of pathogenic material from the host, immune system maturation, and maintenance of intestinal epithelial barrier function (Larabi et al. 2020; Meng et al. 2020). *Lactobacillus* species protect their hosts from intestinal inflammation by regulating the intestinal microbiota (Shin et al. 2019; Kang et al. 2022). In this study, *L. j* and *L. m* pretreatments reshaped the colonic microbiota of LPS-challenged piglets to some extent. SCFAs are crucial metabolites produced by intestinal microorganisms. They can repair TNF-α- and LPS-induced damage to intestinal barrier function (Chen et al. 2017b; Feng et al. 2018). In our animal experiment, the *L. j* and *L. m* interventions elevated the butyric acid concentration, but not the concentration of other SCFAs, in the colonic lumen of the LPS-challenged piglets. Furthermore, butyric acid levels were directly correlated with different microorganisms to varying degrees. The relative abundances of most bacteria increased significantly after the *L. j* and *L. m* interventions, and these bacteria were found to be SCFA-producing bacteria (e.g., *Clostridia_UCG-014_spp* (Zhang et al. 2022), *Olsenella_spp* (Tian et al. 2022), *Bifidobacterium_spp* (Wang et al. 2021), *Blautia_spp* (He et al. 2022), *Rikenellaceae_RC9_gut_group_spp* (Gao et al. 2022), and *Mitsuokella_spp* (Mahmud et al. 2023)). SCFAs can also serve as signaling molecules that activate GPR43 (Koh et al. 2016). Probiotic complexes increase the number of SCFA-producing bacteria and upregulate GPR43 expression. This results in M2 macrophage polarization and inhibition of proinflammatory cytokine expression, thereby restoring intestinal epithelial barrier function (Wang et al. 2020). Consistently, we noted that colonic GPR43 expression was significantly upregulated in the *L.j.* and *L.m.* groups.

We then conducted an in vitro coincubation experiment with SB and macrophages to verify our hypothesis. In a recent study, SB inhibited proinflammatory macrophage polarization both in vitro and in vivo in nonalcoholic

(See figure on next page.)

Fig. 6 Effect of SB or GLPG0974 coincubation with 3D4/2 cells on the TLR4 signaling pathway and tight junction protein expression in LPS-challenged IPEC-J2 cells. **A** GPR43 and Arg1 protein expression of 3D4/2 cells. GPR43 (**B**) and Arg1 (**C**) protein expression analysis in 3D4/2 cells. **D** TLR4, MyD88, p-NF-κB p65, ZO-1, and Occludin protein expression of IPEC-J2 cells. TLR4 (**E**), MyD88 (**F**), p-NF-κB p65 (**G**), ZO-1 (**H**), and Occludin (**I**) protein expression analysis in IPEC-J2 cells. The data are presented as the means ± SEMs ($n = 3$). Differences between the SB and CON groups, $^{**}P < 0.01$, $^{***}P < 0.001$. Differences between the SB + GLPG0974 group and SB group, $\#P < 0.05$, $\#\#\#P < 0.001$. CON, control; LPS, lipopolysaccharide; SB, sodium butyrate

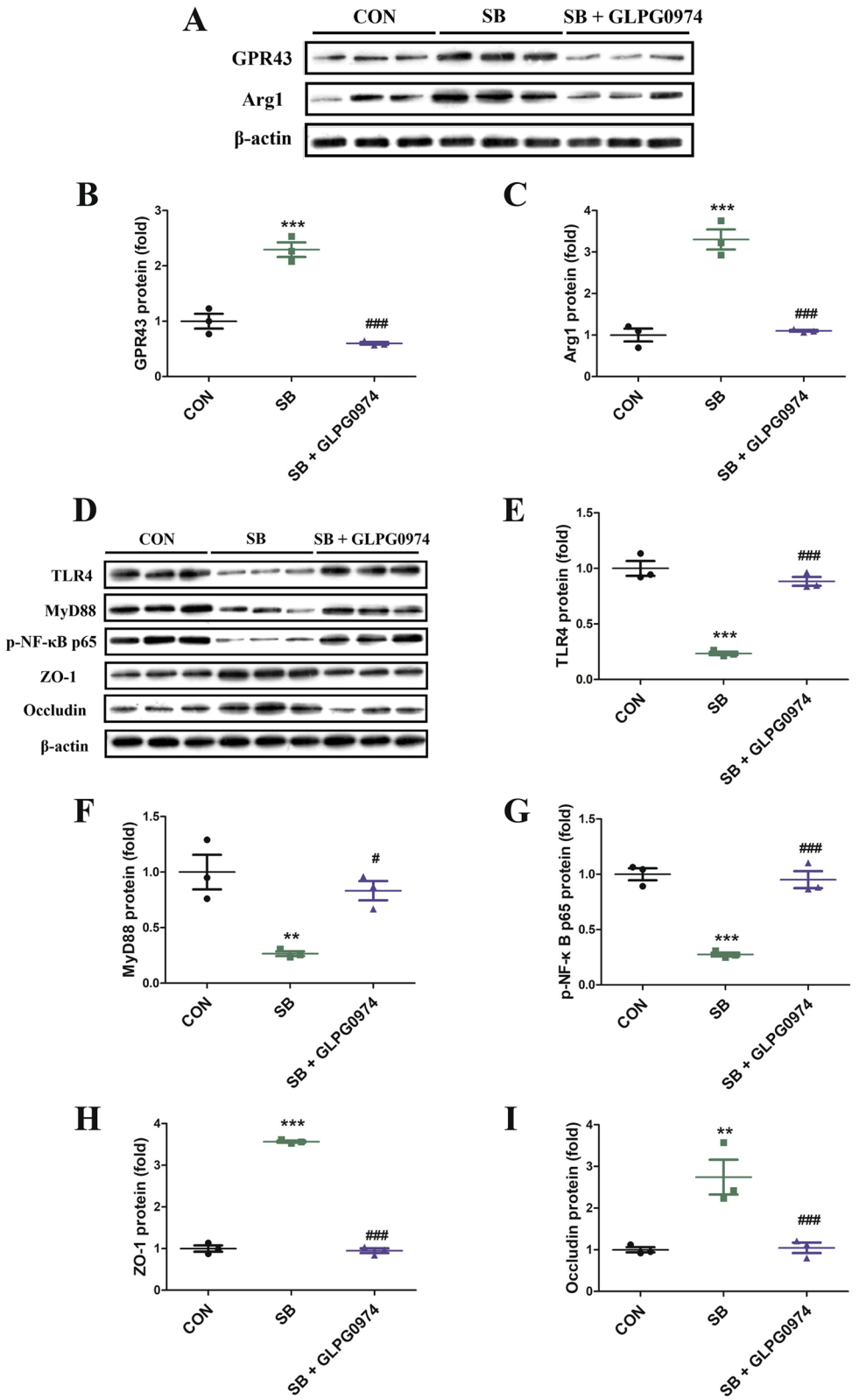

Fig. 6 (See legend on previous page.)

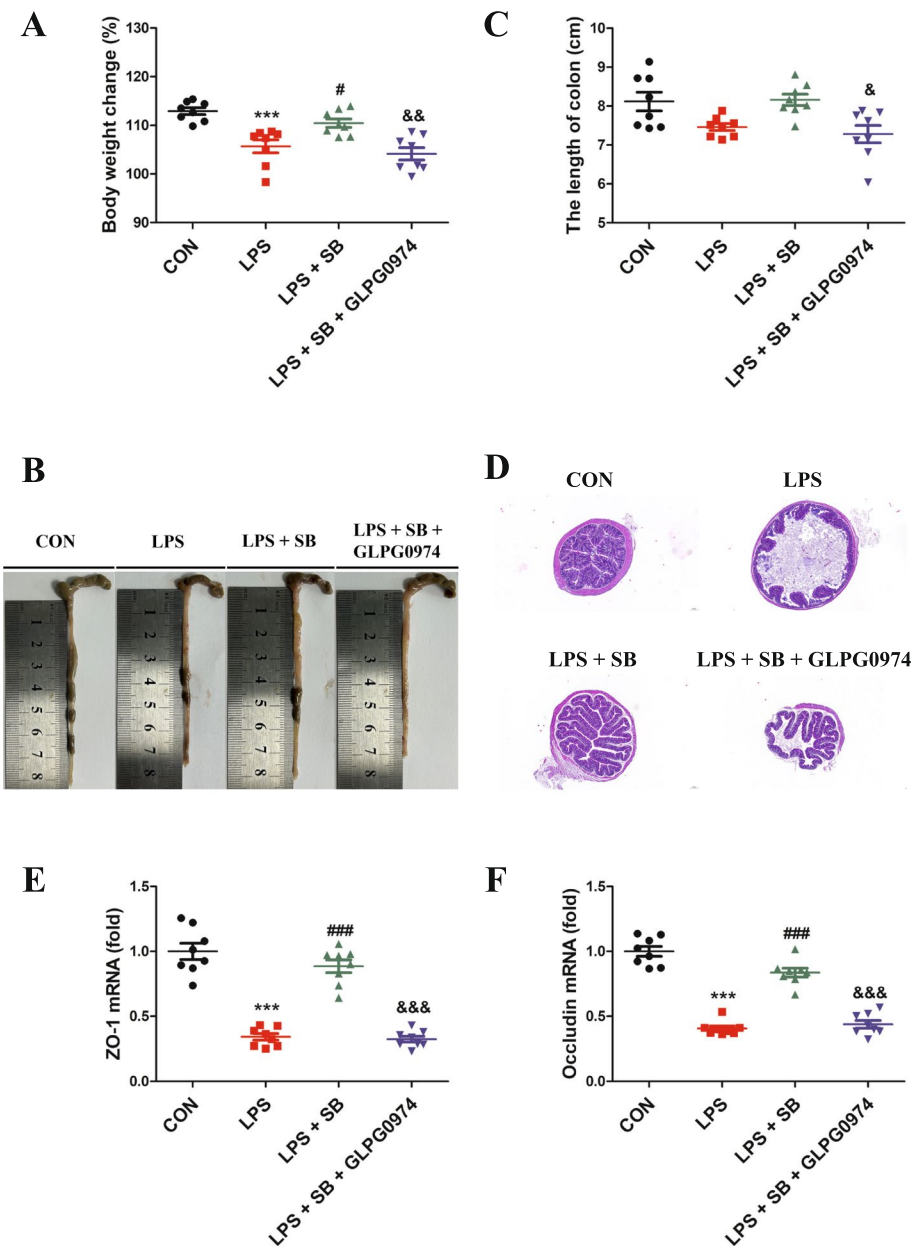

Fig. 7 The effect of SB on colonic barrier function in LPS-challenged mice. **A** Body weight changes of the mice. **B** Mouse colon images. **C** The length of the colon in the mice. **D** Colonic morphological structure after H&E staining. Images of colonic morphology (scale bar = 200 μm). ZO-1 (**E**) and Occludin (**F**) mRNA expression in the colon of mice. The data are presented as the means ± SEMs ($n = 8$). Differences between the LPS and CON groups, ***$P < 0.001$. Differences between the LPS + SB group and the LPS group, #$P < 0.05$, ###$P < 0.001$. Differences between the LPS + SB + GLPG0974 group and LPS + SB group, &$P < 0.05$, &&$P < 0.01$, &&&$P < 0.001$. CON, control; H&E, hematoxylin and eosin; LPS, lipopolysaccharide; SB, sodium butyrate

(See figure on next page.)

Fig. 8 The effect of SB on colonic macrophage polarization and the TLR4 signaling pathway in LPS-challenged mice. Colonic IL-1β (**A**), IL-6 (**B**), TNF-α (**C**), IL-10 (**D**) Colonic iNOS (**E**), Arg1 (**F**), GPR43 (**G**), TLR4 (H), MyD88 (**I**), and NF-κB (**J**) mRNA expression. The data are presented as the means ± SEMs ($n = 8$). Differences between the LPS and CON groups, *$P < 0.001$, ***$P < 0.001$. Differences between the LPS + SB group and the LPS group, ##$P < 0.01$, ###$P < 0.001$. Differences between the LPS + SB + GLPG0974 group and the LPS + SB group, &&$P < 0.01$, &&&$P < 0.001$. Arg1, arginase-1; CON, control; GPR, G protein-coupled receptor; IL, interleukin; iNOS, inducible nitric oxide synthase; LPS, lipopolysaccharide; SB, sodium butyrate; TNF, tumor necrosis factor

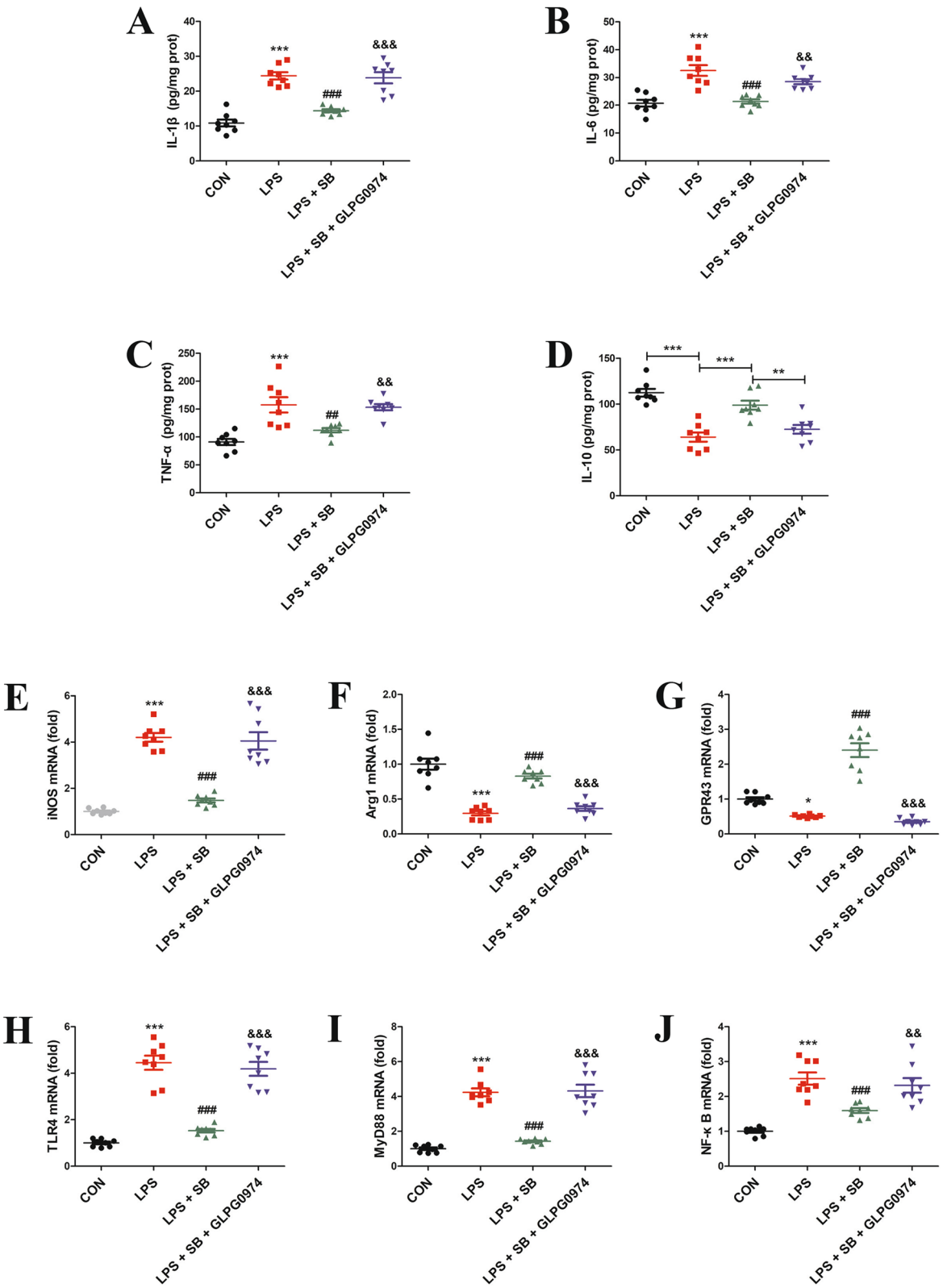

Fig. 8 (See legend on previous page.)

steatohepatitis (NASH) model mice. Moreover, SB intervention reduced the absolute number of hepatic macrophages in NASH mice and increased the number of M2 macrophages. This suggested that SB specifically induces M1 macrophage apoptosis, thereby alleviating NASH (Sarkar et al. 2023). In the present study, SB pretreatment decreased M1 macrophage marker expression but increased M2 macrophage marker expression. It also inhibited proinflammatory cytokine secretion and augmented anti-inflammatory cytokine secretion. Furthermore, GLPG0974 (a GPR43 inhibitor)-pretreated macrophages lost their ability to respond to SB, which suggested that the regulation of macrophage phenotype conversion by SB is GPR43 dependent. Our previous study suggested that extracellular vesicles mitigate intestinal inflammation by modulating macrophage polarization via *L.j* and *L.m*. In the present study, we showed that *L.j* and *L.m* alleviated intestinal inflammation by modulating the SCFA-GPR43-M2 macrophage gut barrier axis. The site of action of extracellular vesicles for alleviating inflammation was the small intestine, whereas the site of action of butyric acid in this study was the large intestine. Based on the physiological characteristics of the different intestinal segments, *Lactobacillus* may act mainly in the form of extracellular vesicles in the small intestine, where the microbiota is relatively scarce, and in the large intestine, where the microbiota is abundant, mainly in the pathway regulating the microbiome as well as metabolites (butyric acid). It is therefore reasonable to speculate that these two mechanisms of regulation operate in parallel.

The molecular mechanisms through which SB-treated macrophages regulate intestinal epithelial barrier function were explored here by establishing a coculture model of macrophages and intestinal epithelial cells. TLRs are specific pattern recognition receptors (PRRs) that activate the TLR4-MyD88-NF-κB cascade signaling pathway following LPS stimulation, thereby initiating cytokine and chemokine production (Lu et al. 2008; Lv et al. 2017). Therefore, targeted inhibition of TLR4-mediated inflammatory signaling pathways effectively controls the inflammatory response. In our coculture system, SB-treated macrophages effectively blocked the expression of the TLR4 signaling pathway but augmented the expression of tight junction proteins in intestinal epithelial cells. However, GLPG0974-treated macrophages did not exert these biological effects on intestinal epithelial cells. In this study, the conclusion that SB promotes M2 macrophage polarization by activating GPR43 and thus enhances intestinal barrier function was validated in a mouse model.

Conclusion

In conclusion, this study showed that *Lactobacillus* (*L. j* and *L. m*) increased the butyric acid concentration by improving the gut microbiota. Butyric acid modulates the macrophage phenotype through activation of GPR43 expression, thereby alleviating the LPS-induced impairment of intestinal barrier function. Notably, GPR43 is necessary for SB to regulate the macrophage phenotype, subsequently allowing SB-treated macrophages to modulate inflammatory signaling pathways and barrier function in intestinal epithelial cells. These findings provide a better understanding of the immunomodulatory effects of probiotics, particularly *Lactobacillus*, on the host gut based on macrophage–intestinal epithelial cell interactions and may contribute to the development of nutritional intervention strategies.

Methods

Animals and sample collection for the piglet experiment

Thirty-two healthy weaned piglets (50% male and 50% female; Duroc × Landrace × Large White; average body weight: 8.53 kg; age: 28 d) were selected for the animal trial. All the piglets were randomized into four groups: the control (CON) group, LPS group, LPS + *L. j* group, and LPS + *L. m* group. For the CON group, the piglets were orally inoculated with PBS for 14 d before they received an intraperitoneal injection of PBS. The LPS group piglets were orally inoculated with PBS for 14 d before they were intraperitoneally injected with LPS (100 μg/kg body weight; Sigma–Aldrich). In the LPS + *L. j* or LPS + *L. m* group, the piglets were orally inoculated with *L. j* (1.2×10^{10} CFU/d) or *L. m* (2.2×10^{10} CFU/d) for 14 d before they were intraperitoneally injected with LPS. *L. j* and *L. m* strains were isolated from the fecal samples of healthy piglets in our laboratory. The piglets were euthanized 4 h after the LPS challenge (Mao et al. 2020). After the piglets were sacrificed, their colonic digesta was collected and stored at −80°C. For histological examination, colonic samples were collected and fixed in 4% paraformaldehyde. The colonic epithelium was separated from the muscular layers and stored at −80°C. Figure 1A presents the in vivo *experimental design*. Throughout the trial, no antibiotics or other medications were given to the piglets. The basal diet of the piglets was formulated according to the NRC (2012). The animal trial was conducted at Tianpeng Husbandry, which is located in Langfang, Hebei Province, China. The experimental procedures were approved by the Institute Animal Care and Use Committee of the Institute of Feed Research of the Chinese Academy of Agricultural Sciences (IFR-CAAS20220922).

Cell culture and treatment

Porcine 3D4/2 macrophages (BeNa Culture Collection, BNCC286806) and IPEC-J2 intestinal epithelial cells (BeNa Culture Collection, BNCC338252) were selected to investigate the effects of sodium butyrate (SB) and GPR43 on LPS-induced inflammation in vitro (Fig. 1B and C). 3D4/2 or IPEC-J2 cells (5×10^5 cells/mL) were incubated with 50 μg/mL SB for 24 h or with 10 nM GLPG0974 (a GPR43 inhibitor) for 3 h. Then, the cells were incubated with 50 μg/mL SB for 24 h, followed by 10 μg/mL LPS for 12 h. For the 3D4/2 and IPEC-J2 cell coculture system, 50 μg/mL SB (24 h) or 10 nM GLPG0974 (3 h) post hoc 50 μg/mL SB (24 h)-pretreated 3D4/2 cells were added to the basolateral compartment of a 6-well plate, and LPS-stimulated (10 μg/mL, 12 h) IPEC-J2 cells were seeded on the apical compartment of 6-well hanging inserts. After 12 h of coculturing, 3D4/2 and IPEC-J2 cells were collected.

Animals and sample collection for the mouse experiment

Thirty-two SPF C57BL/6 mice (aged 6 weeks) were selected and randomly allocated to four groups ($n=8$ per group): (i) the CON group; (ii) the LPS group; (iii) the LPS + SB group; and (iv) the LPS + SB + GLPG0974 group. The CON group mice were fed distilled water for 7 d before they were intraperitoneally injected with PBS. Mice in the LPS group were fed distilled water for 7 d before they were intraperitoneally injected with LPS (5 mg/kg body weight; Sigma–Aldrich). Mice in the LPS + SB group were fed distilled water plus 200 mM SB for 7 d before they received an intraperitoneal injection of LPS. The LPS + SB + GLPG0974 group mice received the same treatments as the LPS + SB group mice, along with oral inoculation of GLPG0974 (10 mg/kg) on days 0 and 4. The mice were euthanized 6 h after the LPS challenge. After the mice were sacrificed, their colonic histological samples and colonic epithelium samples were collected. Figure 1D presents the in vivo experimental design.

Morphological analysis

Hematoxylin and eosin (H&E) staining was conducted according to our previous research (Tao et al. 2019). The colonic epithelial histopathology score was determined using the criteria adapted from our previous study (Tao et al. 2019).

Immunohistochemical analysis

Immunohistochemical (IHC) staining was performed according to our previous study (Tao et al. 2019). The same brown color was selected as the uniform standard for judging all photos by using Image-Pro Plus 6.0 software (Media Cybernetics, Inc., Rockville, MD, USA).

Cytokine measurement

The contents of interleukin (IL)-1β, IL-6, IL-10, and tumor necrosis factor (TNF)-α in the colonic tissues in vivo and in the cellular supernatant in vitro were determined using porcine enzyme-linked immunosorbent assay kits (Shanghai Enzyme-linked Biotechnology Co., Ltd., Shanghai, China).

Bacterial DNA extraction and 16S rRNA amplification, sequencing, and analysis

Total genomic DNA was extracted from the colonic digesta samples by using the QIAamp Fast DNA Stool Mini Kit (Qiagen, Tübingen, Germany). The DNA concentration and quality were determined using a Qubit V. 2.0 fluorometer (Life Technologies, CA, USA). The V3–V4 region of the 16S rRNA gene was amplified using universal primers, pooled in equimolar amounts, and sequenced on the Illumina MiSeq platform to generate 300-bp paired-end reads. Raw reads without barcodes were subjected to quality control by filtering out low-quality reads (Supplemental Table 1). The high-quality reads obtained were imported into QIIME2 as an input. In brief, high-quality sequences were denoised using the DADA2 algorithm and then subjected to taxonomy classification by using the SILVA 132 database. The Majorbio Cloud Platform's free online platform was used for analyzing the data (www.majorbio.com). Correlations were analyzed using Spearman's coefficient.

SCFA measurement

The SCFA profile of the colonic digesta samples was quantified through ion chromatography, according to a previous study (Wu et al. 2021). SCFA analysis was performed using an ion chromatography system (Thermo Fisher Scientific, Waltham, MA, USA).

RNA isolation, cDNA synthesis, and real-time quantitative PCR

Total RNA from the colonic tissues was extracted using TRIzol reagent (Invitrogen). The extracted RNA was quantified using a NanoDrop ND-1000 Spectrophotometer (Thermo, USA). Then, 2 μg of total RNA was treated with RNase-free DNase (M6101; Promega, USA) and reverse transcribed. Subsequently, 2 μL of diluted cDNA was used for real-time PCR. β-actin was selected as a reference gene. Supplemental Table 2 lists all primers selected for the study.

Western blotting

Proteins were extracted from the colonic tissue or cells, quantified, separated through SDS–PAGE, and transferred to nitrocellulose membranes (BioTrace, Pall Co., USA). The membranes were soaked in blocking buffer and incubated with the primary antibody. The next day, the membranes were washed with Tris-buffered saline with Tween (TBST) and incubated with secondary antibodies. Finally, protein expression was recorded and analyzed using an imaging system (Bio-Rad, USA) and Quantity One software (Bio-Rad, USA), respectively. The following antibodies were used for western blotting: HRP-conjugated secondary antibodies (Santa Cruz Biotechnology, goat anti-rabbit (sc-2004)), ZO-1 (Abcam, ab221547), Occludin (Abcam, ab216327), iNOS (Abcam, ab178945), Arg1 (Abcam, ab92274), GPR43 (Proteintech, 19952), TLR4 (Proteintech, 19811-1-AP), MyD88 (CST, 4283), p-NF-κB p65 (CST, 3033), and β-actin (Sigma–Aldrich, A5441).

Statistical analysis

One-way analysis of variance and a post hoc Tukey's test were performed (SPSS version 20.0 for Windows; SPSS Inc., Chicago, IL, USA). All results are presented as the means ± SEMs. Differences were considered statistically significant if $P < 0.05$. The figures included the replicate counts used for statistical analysis.

Abbreviations

ANOVA	One-way analysis of variance
Arg1	Arginase-1
CON	Control
DMEM	Dulbecco's modified Eagle's medium
GPR43	G protein-coupled receptor 43
H&E	Hematoxylin and eosin
HRP	Horseradish peroxidase
IHC	Immunohistochemical
IL	Interleukin
iNOS	Inducible nitric oxide synthase
L. j	*Limosilactobacillus johnsoni*
L. m	*Limosilactobacillus mucosae*
LPS	Lipopolysaccharide
NASH	Nonalcoholic steatohepatitis
PCoA	Principal coordinate analysis
SB	Sodium butyrate
SCFAs	Short-chain fatty acids
TBST	Tris-buffered saline with Tween
TNF	Tumor necrosis factor

Supplementary Information

The online version contains supplementary material available at https://doi.org/10.1186/s44149-024-00125-y.

Supplementary Material 1.

Authors' contributions

The authors' responsibilities were as follows: LXD, ZB, and TSY: designed the research; YY, ZYH, SMZ, FJP, LJJ, FSK, and WZF: conducted the experiments and analyzed the data; TSY: wrote the paper; LXD: had primary responsibility for the final content; and all authors: read and approved the final manuscript.

Funding

This work was supported by the National Nature Science Foundation of China (32272898), the National Key Research and Development Program (2021YFA0805904), and the Fundamental Research Funds for the Central Universities (2662020DKQD004).

Availability of data and materials

The datasets supporting the conclusions of this article are available in the NCBI Sequence Read Archive (SRA) repository (accession number: PRJNA944824).

Declarations

Ethics approval and consent to participate

The trial was conducted at Tianpeng Husbandry, which is located in Langfang, Hebei Province, China. The experimental procedures in this study were approved by the Institute Animal Care and Use Committee of the Institute of Feed Research of the Chinese Academy of Agricultural Sciences (IFR-CAAS20220922).

Competing interests

The authors declare that they have no competing interests.

Received: 8 March 2024 Accepted: 30 April 2024
Published online: 17 June 2024

References

Ayyanna, R., D. Ankaiah, and V. Arul. 2018. Anti-inflammatory and antioxidant properties of probiotic bacterium lactobacillus mucosae AN1 and lactobacillus fermentum SNR1 in *Wistar Albino* Rats. *Frontiers in Microbiology* 9: 3063. https://doi.org/10.3389/fmicb.2018.03063.

Bain, C.C., and A.M. Mowat. 2014. Macrophages in intestinal homeostasis and inflammation. *Immunological Reviews* 260 (1): 102–117. https://doi.org/10.1111/imr.12192.

Chen, J.L., P. Zheng, C. Zhang, B. Yu, J. He, J. Yu, J.Q. Luo, X.B. Mao, Z.Q. Huang, and D.W. Chen. 2017a. Benzoic acid beneficially affects growth performance of weaned pigs which was associated with changes in gut bacterial populations, morphology indices and growth factor gene expression. *Journal of Animal Physiology and Animal Nutrition* 101 (6): 1137–1146. https://doi.org/10.1111/jpn.12627.

Chen, T., C.Y. Kim, A. Kaur, L. Lamothe, M. Shaikh, A. Keshavarzian, and B.R. Hamaker. 2017b. Dietary fiber-based SCFA mixtures promote both protection and repair of intestinal epithelial barrier function in a Caco-2 cell model. *Food & Function* 8 (3): 1166–1173. https://doi.org/10.1039/c6fo01532h.

Chen, Y., W. Cui, X. Li, and H. Yang. 2021. Interaction between commensal bacteria, immune response and the intestinal barrier in inflammatory bowel disease. *Frontiers in Immunology* 12: 761981. https://doi.org/10.3389/fimmu.2021.761981.

Cui, Y., S. Qi, W. Zhang, J. Mao, R. Tang, C. Wang, J. Liu, X.M. Luo, and H. Wang. 2019. Lactobacillus reuteri ZJ617 culture supernatant attenuates acute liver injury induced in mice by lipopolysaccharide. *Journal of Nutrition* 149 (11): 2046–2055. https://doi.org/10.1093/jn/nxz088.

Di Tommaso, N., A. Gasbarrini, and F.R. Ponziani. 2021. Intestinal barrier in human health and disease. *International Journal of Environmental Research and Public Health* 18 (23): 12836. https://doi.org/10.3390/ijerph182312836.

Feng, W., Y. Wu, G. Chen, S. Fu, B. Li, B. Huang, D. Wang, W. Wang, and J. Liu. 2018. Sodium butyrate attenuates diarrhea in weaned piglets and promotes tight junction protein expression in colon in a GPR109A-dependent manner. *Cellular Physiology and Biochemistry* 47 (4): 1617–1629. https://doi.org/10.1159/000490981.

Fu, J., and H. Wu. 2023. Structural mechanisms of NLRP3 inflammasome assembly and activation. *Annual Review of Immunology* 41: 301–316. https://doi.org/10.1146/annurev-immunol-081022-021207.

Gao, Q., G. Sun, J. Duan, C. Luo, C. Yangji, R. Zhong, L. Chen, Y. Zhu, B. Wangdui, and H. Zhang. 2022. Alterations in gut microbiota improve SCFA production and fiber utilization in Tibetan pigs fed alfalfa diet. *Frontiers in Microbiology* 13: 969524. https://doi.org/10.3389/fmicb.2022.969524.

Gensollen, T., S.S. Iyer, D.L. Kasper, and R.S. Blumberg. 2016. How colonization by microbiota in early life shapes the immune system. *Science* 352 (6285): 539–544. https://doi.org/10.1126/science.aad9378.

Han, D., D. Lu, S. Huang, J. Pang, Y. Wu, J. Hu, X. Zhang, Y. Pi, G. Zhang, and J. Wang. 2022. Small extracellular vesicles from Ptpn1-deficient macrophages alleviate intestinal inflammation by reprogramming macrophage polarization via lactadherin enrichment. *Redox Biology* 58: 102558. https://doi.org/10.1016/j.redox.2022.102558.

He, X., C. Yan, S. Zhao, Y. Zhao, R. Huang, and Y. Li. 2022. The preventive effects of probiotic Akkermansia muciniphila on D-galactose/AlCl3 mediated Alzheimer's disease-like rats. *Experimental Gerontology* 170: 111959. https://doi.org/10.1016/j.exger.2022.111959.

Hu, R., H. Lin, M. Wang, Y. Zhao, H. Liu, Y. Min, X. Yang, Y. Gao, and M. Yang. 2021. Lactobacillus reuteri-derived extracellular vesicles maintain intestinal immune homeostasis against lipopolysaccharide-induced inflammatory responses in broilers. *Journal of Animal Science and Biotechnology* 12 (1): 25. https://doi.org/10.1186/s40104-020-00532-4.

Huang, S., S. Hu, S. Liu, B. Tang, Y. Liu, L. Tang, Y. Lei, L. Zhong, S. Yang, and S. He. 2022. Lithium carbonate alleviates colon inflammation through modulating gut microbiota and Treg cells in a GPR43-dependent manner. *Pharmacological Research* 175: 105992. https://doi.org/10.1016/j.phrs.2021.105992.

Isidro, R.A., and C.B. Appleyard. 2016. Colonic macrophage polarization in homeostasis, inflammation, and cancer. *American Journal of Physiology. Gastrointestinal and Liver Physiology* 311 (1): G59-73. https://doi.org/10.1152/ajpgi.00123.2016.

Jia, D.J., Q.W. Wang, Y.Y. Hu, J.M. He, Q.W. Ge, Y.D. Qi, L.Y. Chen, Y. Zhang, L.N. Fan, Y.F. Lin, Y. Sun, Y. Jiang, L. Wang, Y.F. Fang, H.Q. He, X.E. Pi, W. Liu, S.J. Chen, and L.J. Wang. 2022. *Lactobacillus johnsonii* alleviates colitis by TLR1/2-STAT3 mediated CD206(+) macrophages(IL-10) activation. *Gut Microbes* 14 (1): 2145843. https://doi.org/10.1080/19490976.2022.2145843.

Kang, Y., X. Kang, H. Yang, H. Liu, X. Yang, Q. Liu, H. Tian, Y. Xue, P. Ren, X. Kuang, Y. Cai, M. Tong, L. Li, and W. Fan. 2022. *Lactobacillus acidophilus* ameliorates obesity in mice through modulation of gut microbiota dysbiosis and intestinal permeability. *Pharmacological Research* 175: 106020. https://doi.org/10.1016/j.phrs.2021.106020.

Kimura, I., A. Ichimura, R. Ohue-Kitano, and M. Igarashi. 2020. Free fatty acid receptors in health and disease. *Physiological Reviews* 100 (1): 171–210. https://doi.org/10.1152/physrev.00041.2018.

Koh, A., F. De Vadder, P. Kovatcheva-Datchary, and F. Backhed. 2016. From dietary fiber to host physiology: short-chain fatty acids as key bacterial metabolites. *Cell* 165 (6): 1332–1345. https://doi.org/10.1016/j.cell.2016.05.041.

Larabi, A., N. Barnich, and H.T.T. Nguyen. 2020. New insights into the interplay between autophagy, gut microbiota and inflammatory responses in IBD. *Autophagy* 16 (1): 38–51. https://doi.org/10.1080/15548627.2019.1635384.

Li, S.C., W.F. Hsu, J.S. Chang, and C.K. Shih. 2019. Combination of *Lactobacillus acidophilus* and bifidobacterium animalis subsp. lactis shows a stronger anti-inflammatory effect than individual strains in HT-29 cells. *Nutrients* 11 (5): 969. https://doi.org/10.3390/nu11050969.

Li, J., S. Feng, Y. Pi, X. Jiang, X. Li, Z. Zhou, X. Liu, H. Wei, and S. Tao. 2023a. *Limosilactobacillus johnsoni* and *Limosilactobacillus mucosae* and their extracellular vesicles alleviate gut inflammatory injury by mediating macrophage polarization in a lipopolysaccharide-challenged piglet model. *Journal of Nutrition* 153 (8): 2497–2511. https://doi.org/10.1016/j.tjnut.2023.06.009.

Li, J., S. Feng, Z. Wang, J. He, Z. Zhang, H. Zou, Z. Wu, X. Liu, H. Wei, and S. Tao. 2023b. Limosilactobacillus mucosae-derived extracellular vesicles modulates macrophage phenotype and orchestrates gut homeostasis in a diarrheal piglet model. *NPJ Biofilms Microbiomes* 9 (1): 33. https://doi.org/10.1038/s41522-023-00403-6.

Liu, Y., Q. Xu, Y. Wang, T. Liang, X. Li, D. Wang, X. Wang, H. Zhu, and K. Xiao. 2021. Necroptosis is active and contributes to intestinal injury in a piglet model with lipopolysaccharide challenge. *Cell Death & Disease* 12 (1): 62. https://doi.org/10.1038/s41419-020-03365-1.

Lu, Y.C., W.C. Yeh, and P.S. Ohashi. 2008. LPS/TLR4 signal transduction pathway. *Cytokine* 42 (2): 145–151. https://doi.org/10.1016/j.cyto.2008.01.006.

Lv, S., J. Li, X. Qiu, W. Li, C. Zhang, Z.N. Zhang, and B. Luan. 2017. A negative feedback loop of ICER and NF-kappaB regulates TLR signaling in innate immune responses. *Cell Death and Differentiation* 24 (3): 492–499. https://doi.org/10.1038/cdd.2016.148.

Macia, L., J. Tan, A.T. Vieira, K. Leach, D. Stanley, S. Luong, M. Maruya, C. Ian McKenzie, A. Hijikata, C. Wong, et al. 2015. Metabolite-sensing receptors GPR43 and GPR109A facilitate dietary fiber-induced gut homeostasis through regulation of the inflammasome. *Nature Communications* 6: 6734. https://doi.org/10.1038/ncomms7734.

Mahmud, M.R., C. Jian, M.K. Uddin, M. Huhtinen, A. Salonen, O. Peltoniemi, H. Venhoranta, and C. Oliviero. 2023. Impact of intestinal microbiota on growth performance of suckling and weaned piglets. *Microbiology Spectrum* 11 (3): e0374422. https://doi.org/10.1128/spectrum.03744-22.

Mao, J., S. Qi, Y. Cui, X. Dou, X.M. Luo, J. Liu, T. Zhu, Y. Ma, and H. Wang. 2020. *Lactobacillus rhamnosus* GG attenuates lipopolysaccharide-induced inflammation and barrier dysfunction by regulating MAPK/NF-kappaB signaling and modulating metabolome in the piglet intestine. *Journal of Nutrition* 150 (5): 1313–1323. https://doi.org/10.1093/jn/nxaa009.

Meng, Q., Z. Luo, C. Cao, S. Sun, Q. Ma, Z. Li, B. Shi, and A. Shan. 2020. Weaning alters intestinal gene expression involved in nutrient metabolism by shaping gut microbiota in pigs. *Frontiers in Microbiology* 11: 694. https://doi.org/10.3389/fmicb.2020.00694.

Meurens, F., A. Summerfield, H. Nauwynck, L. Saif, and V. Gerdts. 2012. The pig: A model for human infectious diseases. *Trends in Microbiology* 20 (1): 50–57. https://doi.org/10.1016/j.tim.2011.11.002.

Na, Y.R., M. Stakenborg, S.H. Seok, and G. Matteoli. 2019. Macrophages in intestinal inflammation and resolution: A potential therapeutic target in IBD. *Nature Reviews. Gastroenterology & Hepatology* 16 (9): 531–543. https://doi.org/10.1038/s41575-019-0172-4.

Quail, D.F., R.L. Bowman, L. Akkari, M.L. Quick, A.J. Schuhmacher, J.T. Huse, E.C. Holland, J.C. Sutton, and J.A. Joyce. 2016. The tumor microenvironment underlies acquired resistance to CSF-1R inhibition in gliomas. *Science* 352 (6288): aad3018. https://doi.org/10.1126/science.aad3018.

Rodriguez-Sorrento, A., L. Castillejos, P. Lopez-Colom, G. Cifuentes-Orjuela, M. Rodriguez-Palmero, J.A. Moreno-Munoz, D. Luise, P. Trevisi, and S.M. Martin-Orue. 2021. Effects of the administration of bifidobacterium longum subsp. infantis CECT 7210 and lactobacillus rhamnosus HN001 and their synbiotic combination with galacto-oligosaccharides against enterotoxigenic *Escherichia coli* F4 in an early weaned piglet model. *Frontiers in Microbiology* 12: 642549. https://doi.org/10.3389/fmicb.2021.642549.

Sarkar, A., P. Mitra, A. Lahiri, T. Das, J. Sarkar, S. Paul, and P. Chakrabarti. 2023. Butyrate limits inflammatory macrophage niche in NASH. *Cell Death & Disease* 14 (5): 332. https://doi.org/10.1038/s41419-023-05853-6.

Shin, D., S.Y. Chang, P. Bogere, K. Won, J.Y. Choi, Y.J. Choi, H.K. Lee, J. Hur, B.Y. Park, Y. Kim, and J. Heo. 2019. Beneficial roles of probiotics on the modulation of gut microbiota and immune response in pigs. *PLoS One* 14 (8): e0220843. https://doi.org/10.1371/journal.pone.0220843.

Sica, A., M. Erreni, P. Allavena, and C. Porta. 2015. Macrophage polarization in pathology. *Cellular and Molecular Life Sciences* 72 (21): 4111–4126. https://doi.org/10.1007/s00018-015-1995-y.

Tang, X., K. Xiong, R. Fang, and M. Li. 2022. Weaning stress and intestinal health of piglets: A review. *Frontiers in Immunology* 13: 1042778. https://doi.org/10.3389/fimmu.2022.1042778.

Tao, S., Y. Bai, T. Li, N. Li, and J. Wang. 2019. Original low birth weight deteriorates the hindgut epithelial barrier function in pigs at the growing stage. *The FASEB Journal* 33 (9): 9897–9912. https://doi.org/10.1096/fj.201900204RR.

Tian, B., Y. Geng, P. Wang, M. Cai, J. Neng, J. Hu, D. Xia, W. Cao, K. Yang, and P. Sun. 2022. Ferulic acid improves intestinal barrier function through altering gut microbiota composition in high-fat diet-induced mice. *European Journal of Nutrition* 61 (7): 3767–3783. https://doi.org/10.1007/s00394-022-02927-7.

Vieira, A.T., L. Macia, I. Galvao, F.S. Martins, M.C. Canesso, F.A. Amaral, C.C. Garcia, K.M. Maslowski, E. De Leon, D. Shim, J.R. Nicoli, J.L. Harper, M.M. Teixeira, and C.R. Mackay. 2015. A role for gut microbiota and the metabolite-sensing receptor GPR43 in a murine model of gout. *Arthritis & Rhematology* 67 (6): 1646–1656. https://doi.org/10.1002/art.39107.

Viola, M.F., and G. Boeckxstaens. 2021. Niche-specific functional heterogeneity of intestinal resident macrophages. *Gut* 70 (7): 1383–1395. https://doi.org/10.1136/gutjnl-2020-323121.

Wang, Y., Y. Wu, J. Sailike, X. Sun, N. Abuduwaili, H. Tuoliuhan, M. Yusufu, and X.H. Nabi. 2020. Fourteen composite probiotics alleviate type 2 diabetes through modulating gut microbiota and modifying M1/M2 phenotype macrophage in db/db mice. *Pharmacological Research* 161: 105150. https://doi.org/10.1016/j.phrs.2020.105150.

Wang, Z., Y. Bai, Y. Pi, W.J.J. Gerrits, S. de Vries, L. Shang, S. Tao, S. Zhang, D. Han, Z. Zhu, and J. Wang. 2021. Xylan alleviates dietary fiber

deprivation-induced dysbiosis by selectively promoting Bifidobacterium pseudocatenulatum in pigs. *Microbiome* 9 (1): 227. https://doi.org/10.1186/s40168-021-01175-x.

Wang, C., S. Wei, B. Liu, F. Wang, Z. Lu, M. Jin, and Y. Wang. 2022. Maternal consumption of a fermented diet protects offspring against intestinal inflammation by regulating the gut microbiota. *Gut Microbes* 14 (1): 2057779. https://doi.org/10.1080/19490976.2022.2057779.

Wu, Z., S. Huang, T. Li, N. Li, D. Han, B. Zhang, Z.Z. Xu, S. Zhang, J. Pang, S. Wang, G. Zhang, J. Zhao, and J. Wang. 2021. Gut microbiota from green tea polyphenol-dosed mice improves intestinal epithelial homeostasis and ameliorates experimental colitis. *Microbiome* 9 (1): 184. https://doi.org/10.1186/s40168-021-01115-9.

Wyns, H., E. Meyer, E. Plessers, A. Watteyn, T. van Bergen, S. Schauvliege, S. De Baere, M. Devreese, P. De Backer, and S. Croubels. 2015. Modulation by gamithromycin and ketoprofen of in vitro and in vivo porcine lipopolysaccharide-induced inflammation. *Veterinary Immunology and Immunopathology* 168 (3–4): 211–222. https://doi.org/10.1016/j.vetimm.2015.09.014.

Xia, W., I. Khan, X.A. Li, G. Huang, Z. Yu, W.K. Leong, R. Han, L.T. Ho, and W.L. Wendy Hsiao. 2020. Adaptogenic flower buds exert cancer preventive effects by enhancing the SCFA-producers, strengthening the epithelial tight junction complex and immune responses. *Pharmacological Research* 159: 104809. https://doi.org/10.1016/j.phrs.2020.104809.

Xia, B., R. Zhong, W. Wu, C. Luo, Q. Meng, Q. Gao, Y. Zhao, L. Chen, S. Zhang, X. Zhao, and H. Zhang. 2022. Mucin O-glycan-microbiota axis orchestrates gut homeostasis in a diarrheal pig model. *Microbiome* 10 (1): 139. https://doi.org/10.1186/s40168-022-01326-8.

Xie, Z., M. Li, M. Qian, Z. Yang, and X. Han. 2022. Co-cultures of *Lactobacillus acidophilus* and *Bacillus subtilis* enhance mucosal barrier by modulating gut microbiota-derived short-chain fatty acids. *Nutrients* 14 (21): 4475. https://doi.org/10.3390/nu14214475.

Yang, G.Y., B. Xia, J.H. Su, T. He, X. Liu, L. Guo, S. Zhang, Y.H. Zhu, and J.F. Wang. 2020. Anti-inflammatory effects of *Lactobacillus johnsonii* L531 in a pig model of *Salmonella Infantis* infection involves modulation of CCR6(+) T-cell responses and ER stress. *Veterinary Research* 51 (1): 26. https://doi.org/10.1186/s13567-020-00754-4.

Zhang, X., M. Akhtar, Y. Chen, Z. Ma, Y. Liang, D. Shi, R. Cheng, L. Cui, Y. Hu, A.A. Nafady, A.R. Ansari, E.M. Abdel-Kafy, and H. Liu. 2022. Chicken jejunal microbiota improves growth performance by mitigating intestinal inflammation. *Microbiome* 10 (1): 107. https://doi.org/10.1186/s40168-022-01299-8.

Publisher's Note